An investigation of "A kinetic model of continuous radiation damage to populations of cells"

Ronan Bottoms

June 5th, 2024

Abstract

A group of researchers has published significant work in the past few years on a model of the cellular dynamics of cancer under continuous radiation damage. While this model shows much promise through a robust fit to experimental data, the dynamics of the model are not explored in detail. In this paper, we look closer at the dynamics of the model to ascertain whether any details may have been missed. We do this through a fixed point and bifurcation analysis focused on the radiation dose followed by numerical simulations. Additionally, the model is presented in the form of a coupled set of ODEs. We look to further this model by formulating analogous SDEs and perform numerical simulations of the results.

1 Introduction

The most common way to treat cancer in a patient is through radiation therapy. A radioactive isotope is injected into the patient and causes the DNA of the cancerous cells to break down, resulting in death of the cancerous cells. In a paper by Neira, Gago-Arias, Guiu-Souto, and Pardo-Montero (2020), a model is introduced for the "kinetics of populations of tumor cells" undergoing continuous radiation therapy. The model consists of three categories of cells: healthy (N), sub-lethally damaged (N_s), and doomed cells (N_d). All cells reproduce with different rates logistically toward a fixed saturation population for the entire tumor. Healthy cells damaged by radiation can become sub-lethally damaged or lethally damaged (doomed). Sub-lethally damaged cells can repair themselves and become healthy, whereas doomed cells cannot and eventually die. Since the radiation applied is continuous, sub-lethally damaged cells can also be further damaged and become doomed.

This simple model has a potential for exciting applications. However, the paper does not thoroughly investigate the dynamics of the model. Additionally, two simplifications are offered to the model that appear to change the dynamics of the model potentially significantly. In this report, we investigate the dynamics of this continuous dose rate model and its two simplifications. Using parameter values obtained from figures in the model's paper we perform simulations of all three models and compare their dynamics. Further, we attempt to reformulate the ODEs of the model as stochastic differential equations (SDEs) and perform stochastic simulations of the results.

2 Materials and methods

2.1 The general model

The model described above has the following ODE representation.

$$\frac{dN}{dt} = \lambda N\left[1 - \frac{(N + N_s + N_d)}{N_{sat}}\right] + \mu N_s - (a+b)r(t)N \tag{1}$$

$$\frac{dN_s}{dt} = \lambda_s N_s\left[1 - \frac{(N + N_s + N_d)}{N_{sat}}\right] + br(t)N - \mu N_s - (a+b)r(t)N_s \tag{2}$$

$$\frac{dN_d}{dt} = \lambda_d N_d\left[1 - \frac{(N + N_s + N_d)}{N_{sat}}\right] + ar(t)N + (a+b)r(t)N_s - \gamma N_d \tag{3}$$

Here, healthy cells grow with a rate λ, sub-lethally damaged cells with a rate λ_s, and doomed cells with a rate λ_d. The saturation population of the tumor is denoted by N_{sat}. The continuous radiation dose is the time dependent quantity $r(t)$. Healthy cells are damaged lethally with rate a and sub-lethally with rate b. Further, sub-lethally damaged cells that are again damaged either lethally or sub-lethally become doomed. Sub-lethally damaged cells repair themselves with a rate μ and doomed cells die at a rate γ.

We begin by performing fixed-point analysis of the general model. In order to simplify computation, we first perform the following substitution: we note that

$$\left[1 - \frac{(N + N_s + N_d)}{N_{sat}}\right] =: \rho$$

appears in each of the three differential equations. By multiplying (1) by $\lambda_d\lambda_s N_d N_s$, (3) by $\lambda\lambda_s N N_s$, and (2) by $\lambda\lambda_d N N_d$, we obtain

$$0 = \lambda\lambda_s\lambda_d N N_s N_d\rho + \lambda_d\lambda_s\mu N_d N_s^2 - \lambda_d\lambda_s(a+b)r(t)NN_sN_d \tag{4}$$
$$0 = \lambda\lambda_s\lambda_d N N_s N_d\rho + \lambda\lambda_s a r(t)N^2N_s + \lambda\lambda_s(a+b)r(t)NN_s^2 - \lambda\lambda_s\gamma NN_sN_d \tag{5}$$
$$0 = \lambda\lambda_s\lambda_d N N_s N_d\rho + \lambda\lambda_d b r(t)N^2N_d - \lambda\lambda_d\mu NN_sN_d - \lambda\lambda_d(a+b)r(t)NN_sN_d \tag{6}$$

Then by moving the saturation term $\lambda\lambda_s\lambda_d N N_s N_d\rho$ to the LHS and setting all the equations equal, we obtain the following equivalent system of equations.

$$\lambda_d\lambda_s\mu N_d N_s^2 - \lambda_d\lambda_s(a+b)r(t)NN_sN_d = \lambda\lambda_s a r(t)N^2N_s + \lambda\lambda_s(a+b)r(t)NN_s^2 - \lambda\lambda_s\gamma NN_sN_d \tag{7}$$

$$\begin{aligned}\lambda\lambda_s a r(t)N^2N_s + \lambda\lambda_s(a+b)r(t)NN_s^2 - \lambda\lambda_s\gamma NN_sN_d = \\ \lambda\lambda_d b r(t)N^2N_d - \lambda\lambda_d\mu NN_sN_d - \lambda\lambda_d(a+b)r(t)NN_sN_d\end{aligned} \tag{8}$$

$$\lambda\lambda_d b r(t)N^2N_d - \lambda\lambda_d\mu NN_sN_d - \lambda\lambda_d(a+b)r(t)NN_sN_d = \lambda_d\lambda_s\mu N_d N_s^2 - \lambda_d\lambda_s(a+b)r(t)NN_sN_d \tag{9}$$

These equations were then be solved using Mathematica. The solutions are the origin and a pair of curves that depend on the number of sub-lethally damaged cells. We determined through substitution of feasible parameters that one of the curves always yields a negative number of healthy cells and is thus infeasible for physical situations. The other conjugate curve, however, is an attractor in the domain where the number of healthy cells is positive. The full solutions are shown in Figure 7 of the supplemental material.

We can then compute the Jacobian of the system to determine the stability of these fixed points and curves. Using (1), (2), and (3), we compute

$$J = \begin{bmatrix} J_1 \\ J_2 \\ J_3 \end{bmatrix} \tag{10}$$

where

$$J_1 = \begin{bmatrix} \lambda - \frac{\lambda}{N_{sat}}(2N + N_s + N_d) - (a+b)r & -\frac{\lambda}{N_sat}N + \mu & -\frac{\lambda}{N_{sat}} \end{bmatrix} \tag{11}$$
$$J_2 = \begin{bmatrix} -\frac{\lambda_s}{N_{sat}}N_s + br & \lambda_s - \lambda_s N_{sat}(N + 2N_s + N_d) - \mu - (a+b)r & -\lambda_s N_{sat} N_s \end{bmatrix} \tag{12}$$
$$J_3 = \begin{bmatrix} -\lambda_d N_{sat} + ar & -\lambda_d N_{sat} N_d + (a+b)r & \lambda_d - \lambda_d N_{sat}(N + N_s + 2N_d) - \gamma \end{bmatrix} \tag{13}$$

2.2 Simplifying assumptions

The authors "consistently consider that only viable cells can proliferate and that the radiosensitivity of viable and sub-lethally damaged cells is the same (same a and b parameters in [the] model)" and "certainly, this has to be considered an approximation". Following these assumptions, the effective simplified model is

$$\frac{dN}{dt} = \lambda N\left[1 - \frac{(N + N_s + N_d)}{N_{sat}}\right] + \mu N_s - (a+b)r(t)N \tag{14}$$

$$\frac{dN_s}{dt} = br(t)N - \mu N_s - (a+b)r(t)N_s \tag{15}$$

$$\frac{dN_d}{dt} = ar(t)N + (a+b)r(t)N_s - \gamma N_d \tag{16}$$

where $\lambda_s, \lambda_d = 0$. Despite claiming that they set $a = b$, they kept them different for the two cell types we will be concerned with, Patu-8988T and Dan-G. We have consequently excluded setting $a = b$ equal above.

It is a reasonable expectation that the dynamics of the system under these simplifying assumptions are different from those of the full model. Indeed, by solving the system of equations above using Mathematica, we find that the fixed lines of the full model are reduced to points, one positive and one negative for values of healthy cell populations. The full results are shown in Figure 8 of the supplemental material. How close an approximation this simplification is to the general model will be investigated further in the Results section.

We can additionally compute the Jacobian of the simplified model to determine the stability of the fixed points. We first expand (14) as

$$\lambda N - \frac{\lambda}{N_{sat}}(N^2 + NN_s + NN_d) + \mu N_s - (a+b)rN$$

Then taking derivatives,

$$J = \begin{bmatrix} \lambda - \frac{\lambda}{N_{sat}}(2N + N_s + N_d) - (a+b)r & -\frac{\lambda}{N_{sat}}N + \mu & -\frac{\lambda}{N_{sat}}N \\ br & -\mu - (a+b)r & 0 \\ ar & (a+b)r & -\gamma \end{bmatrix} \tag{17}$$

2.3 LQ limit

The authors also offer a further reduced version of the model. In this reduced case the dose rate of radiation is "fast compared to typical repair times... [so that] we can ignore the effect of sub-lethal damage repair" and doomed cells do not proliferate or die. The dose rate is assumed to be a constant $r(t) = r$. We can then make the substitution $a \cdot r(t) = a \cdot r =: a'$ and similarly $b \cdot r =: b'$.

$$\frac{dN}{dt} = -(a' + b')N \tag{18}$$

$$\frac{dN_s}{dt} = b'N - (a' + b')N_s \tag{19}$$

$$\frac{dN_d}{dt} = a'N + (a' + b')N_s \tag{20}$$

We observe that the death term has been dropped from the doomed cell equation, and all sub-lethal repair terms involving a μ have been removed. The only simplification that was not addressed by the authors is the removal of the logistic growth term from the equation for healthy cells. Indeed, this is an important modification that requires justification.

Now again consider the changes in the fixed points of the system as compared to the general and simplified models. We notice that N_d does not influence N nor N_s, so it can be decoupled from the system. From quick inspection it is apparent that the only fixed point of this reduced system is $(N, N_s) = (0, 0)$. This has the Jacobian

$$\begin{bmatrix} -(a' + b') & 0 \\ b' & -(a' + b') \end{bmatrix}$$

which has eigenvalues $\lambda_1 = \lambda_2 = \lambda = -(a' + b')$. The dimension of the corresponding eigenspace is the nullity of the matrix

$$\begin{bmatrix} -(a' + b') & 0 \\ b' & -(a' + b') \end{bmatrix} + \begin{bmatrix} a' + b' & 0 \\ 0 & a' + b' \end{bmatrix} = \begin{bmatrix} 0 & 0 \\ b & 0 \end{bmatrix} \tag{21}$$

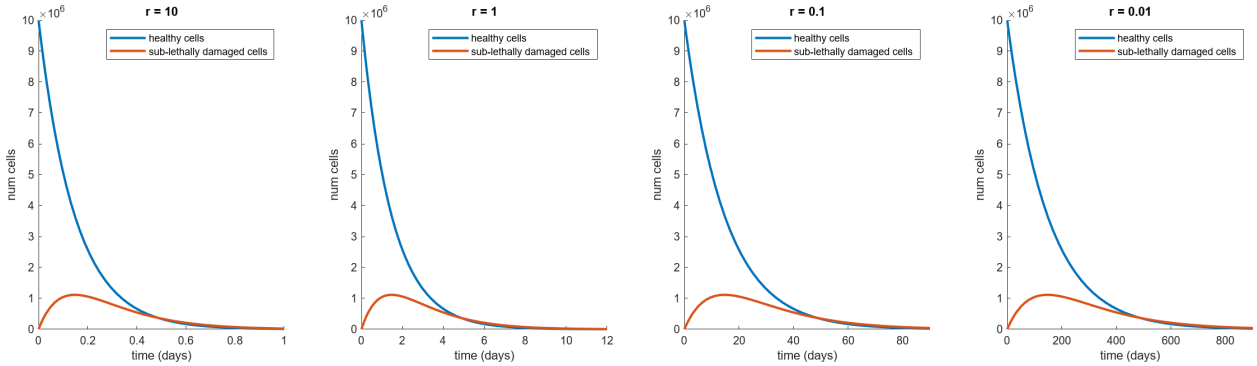

Figure 1: Numerical simulations of the number of healthy and sub-lethally damaged cells using the reduced model for various values of a constant dose rate r starting from a population of 10^6 healthy cells. We observe that the origin is indeed an attractor under all shown values of r.

which is 1 for $b' \neq 0$, implying that this fixed point is degenerate.

We note that since a and b are defined to be rates of radiation damage, they are by definition always non-negative quantities. Since the radiation dosage is also always non-negative, the quantity $a' + b'$ is always *positive* (as both a and b zero implies that the radiation has no effect on the tumor). This implies that the eigenvalues of this system are always negative, and thus the fixed point at the origin is *always* a degenerate attractor. Since degeneracy can contradict the results of linearization, we confirmed that the origin is an attractor numerically using `ode45` simulations in MATLAB for various values of r in Figure 1.

This reduced model is introduced as the "LQ-limit: *closed-form analytical solution...*". The authors seemingly derive this reduction in order to elucidate similarities between their model and the Curtis (1986) model and the LQ model (Lea and Catcheside 1942, Kellerer and Rossi 1974, Fowler 1989). However, as seen from the fixed point analysis, this reduction collapses an entire curve of fixed points to a single (degenerate) attractor at the origin, wildly altering the dynamics of their original model. How accurate a representation this reduction is for their model and whether this is a valid comparison is up to interpretation.

2.4 Comparison using cell parameters

To continue the analysis further, it is necessary to fix several of the parameters of the model. For our purposes, we only allow the radiation term to be time dependent. All other parameters are considered intrinsic properties of the patient's system. We investigate two different parameter regimes: Patu-8988T[1] and Dan-G cells, the same lineages of cells that were investigated extensively in the paper. The paper fixes the radiation damage rates and the death rate of the doomed cells and considers variations in the growth rate of healthy cells and the sub-lethal repair rates of sub-lethally damaged cells. However, as we are investigating the differences between the general and simplified models, we fix λ and μ as one of the possible sets of values they investigated. For our investigation, we choose $\lambda = 0.139$ and $\mu = 15.84$.

Patu-8988T cells are characterized by the following set of parameters:

$$a = 0.0$$
$$b = 0.664$$
$$\gamma = 0.069$$

These cells do not experience any lethal damage from radiation. Healthy cells must first become sub-lethally damaged, and then damaged again in order to become doomed.

Having fixed these parameters, we are now able to comment on the values of the radiation r that affect the feasibility of the fixed points of the simplified model. For feasibiliy, we are interested in at what values

[1]This lineage of cells comes from a pancreatic adenocarcinoma and carries the KRAS and TP53 mutations discussed frequently in class.
`https://www.dsmz.de/collection/catalogue/details/culture/ACC-162`

of r is the fixed point for healthy cells greater than 0, indicating an attractor that increases the size of the tumor. Using Mathematica, we selected the positive fixed point of the simplified model and solved for what values of r the healthy cell population fixed point becomes positive. For Patu-8988T, the fixed point coordinate for the population of healthy cells is given by

$$N = -\frac{4.96403 \times 10^{11} \left(0.440896r^2 - 0.092296r - 1.74306\right)}{0.440896r^2 + 0.091632r + 0.86526} \tag{22}$$

which was greater than 0 for $r < 2.09575$. Thus for radiation levels greater than this value, the non-origin fixed point corresponds to a negative value of healthy cells, and so the fixed point at the origin dominates the behavior of the system and drives the number of healthy cells to 0. For radiation levels less than this value, the tumor experiences growth as it is pulled to the positive attractor.

Dan-G cells are characterized by

$$a = 0.473$$
$$b = 0.206$$
$$\gamma = 0.069$$

These cells experience lethal damage at a much greater rate than sub-lethal damage, indicating a greater radiation sensitivity. The fixed point coordinate for the population of healthy cells is given by

$$N = -\frac{4.96403 \times 10^{11} \left(0.461041r^2 + 5.83704r - 1.74306\right)}{0.461041r^2 + 5.99248r + 0.86526} \tag{23}$$

which was greater than 0 for $r < 0.291891$.

2.5 Implementation

To investigate differences between the general and simplified model, we will look at two different sets of parameters for λ_s and λ_d. As there are many permutations possible, we considered only the pairs ($\lambda_s = 0.139 = \lambda, \lambda_d = 5.55 \cdot 10^{-3}$) and ($\lambda_s = 0.0695, \lambda_d = 3.17 \cdot 10^{-2}$). These values were taken from the supplemental material of a paper that built upon the model under scrutiny by many of the same authors (Gago-Arias, Neira, Terragni, and Pardo-Montero 2021). In that paper, they always used that $\lambda = \lambda_s$, so we followed suit, and the values for λ_d were taken from fits to Grave's hyperthiroidism and DTC local recurrence. In the absence of other relevant data, it seems pertinent to use parameter values that were fit using a similar model.

Further, in the explicit derivation of the fixed points and corresponding stabilities, terms proportional to the saturation population of the tumor appeared. While setting the saturation population equal to infinity in the numerical simulations to represent unbounded growth makes sense, this caused errors when solving analytically. For our purposes, we set the saturation value $N_{sat} = 10^{12}$, a quantity that the tumor should not reasonably be able to attain as the entire human body contains only several trillion cells.

Unfortunately, the authors of the paper failed to clearly state exactly what curve they used for modeling the continuous radiation dose. They say that "dose rate curves were reconstructed by using pharmacokinetic curves presented in" the article by Baiu *et al* (2018). However, we found little evidence of exact curves in that article, leaving us with no way to exactly duplicate the results of the paper. It would have been pertinent for the authors to include the exact curves they used when modeling. To approximate what they did, we consider doses of ^{133}I in two different ways: first by direct injection into the tumor with no uptake time, and by injection into the surrounding region with uptake time. The former is given by

$$r_1(t) = d\left(\frac{1}{2}\right)^{t/8} \tag{24}$$

where d is the initial dose. We use that the half life of ^{133}I is 8 days. The latter is given by the following

$$r_2(t) = d - d\left(\frac{1}{2}\right)^{t/8} \tag{25}$$

so that the dosage is absorbed over a period of several days into the tumor. This more closely matches what the authors of the paper seem to have been using, but without more advanced biological knowledge we are left to speculate.

The general and simplified model were simulated in MATLAB using the `ode45` routine. First, we investigated whether the fixed points of the simplified model lay on the fixed line of the general model. Next, we checked that the values of r that caused tumor suppression are not only correct but worked for both models. This was done using the uptake radiation model (25) in order to keep the cumulative dose high. Finally, we plotted simulations of both the general and simplified model for different initial dosages of radiation for the direct dosage equation (24) to investigate how qualitatively different the simplification is from the general model.

3 Results

3.1 Fixed curves versus fixed points

In Figure 2 we plotted the fixed curves of the general model and the fixed points of the simplified model for both Patu-8988T and Dan-G cells for both (λ_s, λ_d) parameter sets.

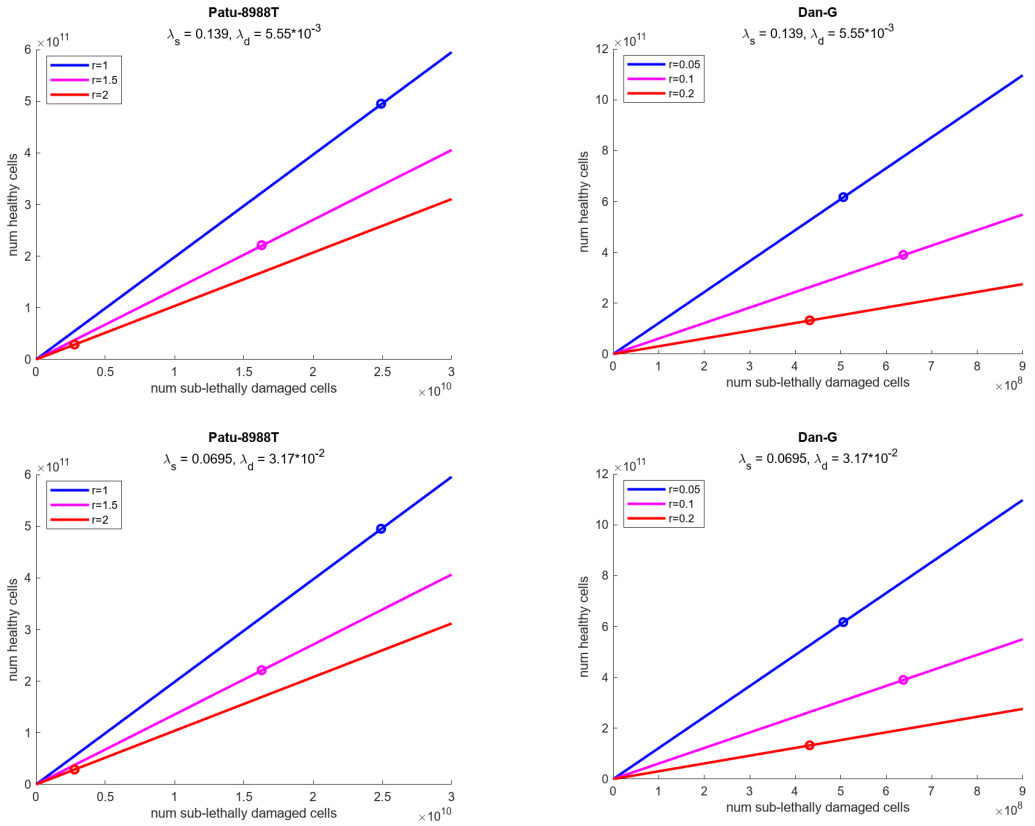

Figure 2: Fixed curves of the general model (solid lines) and fixed points of the simplified model (o marker) for three different radiation values for which the coordinate for the number of healthy cells is positive.

We can see indeed that the fixed points of the simplified model lie on the fixed line of the general model. Only values of the radiation for which the fixed point was positive were considered, for if the fixed point was negative the origin would be the closest attractor. From supplemental investigation, we confirmed that for negative values of healthy cells, the fixed point follows the negative fixed curve as well. To satisfy this

curiosity, one can view for themselves the dynamics for one parameter set at `https://www.desmos.com/calculator/jk3evhn0qk`.

3.2 Radiation values for origin bifurcation

Next we plotted the curves for all three types of cells (healthy, sub-lethally damaged, and doomed) under the uptake radiation curve (25). Values of r were chosen on both sides of the bifurcation value.

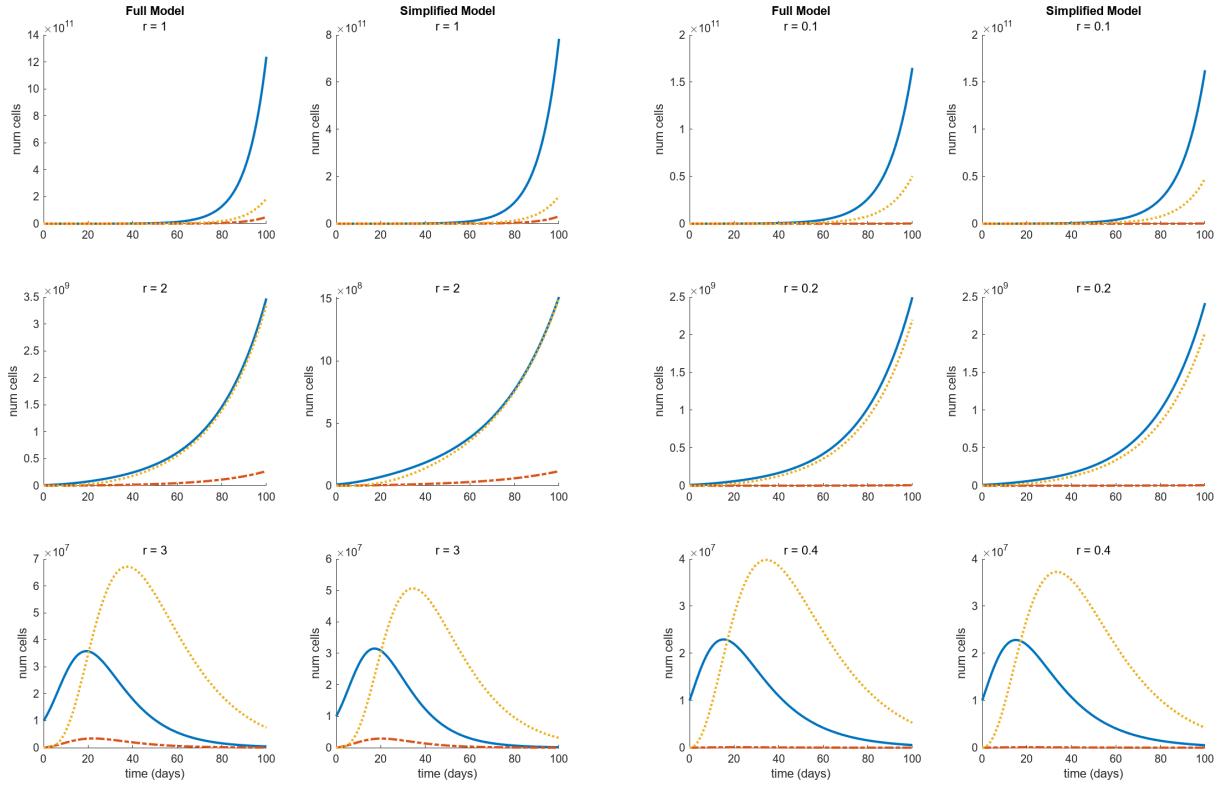

Figure 3: Populations of healthy cells (solid line -), sub-lethally damaged cells (dot-dashed line -.), and doomed cells (dotted line :) for different values of r using the uptake radiation curve, ($\lambda_s = 0.139, \lambda_d = 5.55 \cdot 10^{-3}$).

Recall from equation (22) that the bifurcation value for r in the simplified model was $r = 2.09575$ and from (23) the value was $r = 0.291891$. In Figure 3, we observe that between the second and third rows, the radiation value for both cell types crosses the bifurcation value and subsequently the fixed point at the origin becomes an attractor. Of mention is that this occurs for *both* the general model and simplified model. Further, from a cursory view of the figure we can see that in general the simplified model is a remarkable approximation to the general model. The non-zero growth rate for the doomed cells lends to a slight increase in the number of doomed cells visible between the first and second columns of each cell type, but overall the simplified model closely follows the dynamics of the general model.

One aberrant observation, however, is that for both types of cells the sub-lethally damaged population is miniscule compared to both healthy and doomed. This is especially curious in the case of Patu-8988T cells which have a lethal damage rate of 0. This would suggest that the sub-lethally damaged population should be greater than the lethally damaged doomed one, but the simulations suggest that the reverse occurs. We hypothesized that the high sub-lethal repair rate μ may be contributing to this observed small population size. To test this, we plotted simulations of Patu-8988T cells using the simplified model and the

uptake dosage curve with a fixed dose amount of $r = 2$ for different values of μ in Figure 4. We found that indeed lowering the repair rate caused the population size of the sub-lethally damaged cells to increase and interestingly the bifurcation value for r to decrease.

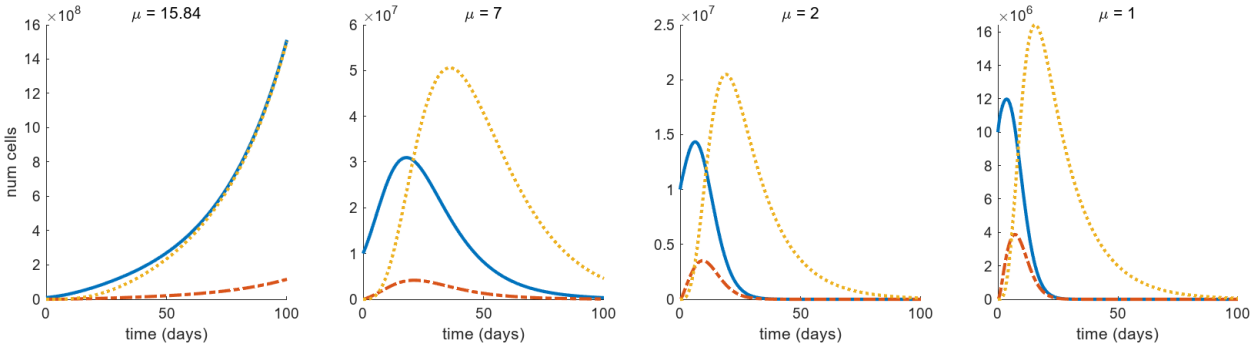

Figure 4: Populations of healthy cells (solid line -), sub-lethally damaged cells (dot-dashed line -.), and doomed cells (dotted line :) for the simplified model for different values of the sub-lethal repair rate μ with other parameters (including r) fixed, ($\lambda_s = 0.139, \lambda_d = 5.55 \cdot 10^{-3}$).

3.3 General comparison

Finally, we plotted Patu-8988T and Dan-G cell populations for both the general and simplified models for several radiation dosages for the dose injection function (24) to observe how closely the simplified model followed the general. The results are show in Figure 5.

Overall, the trajectories of all the populations for both cell populations were remarkably similar, if not nearly identical, to those of the general model. This shows that the simplification the authors performed is a valid simplification.

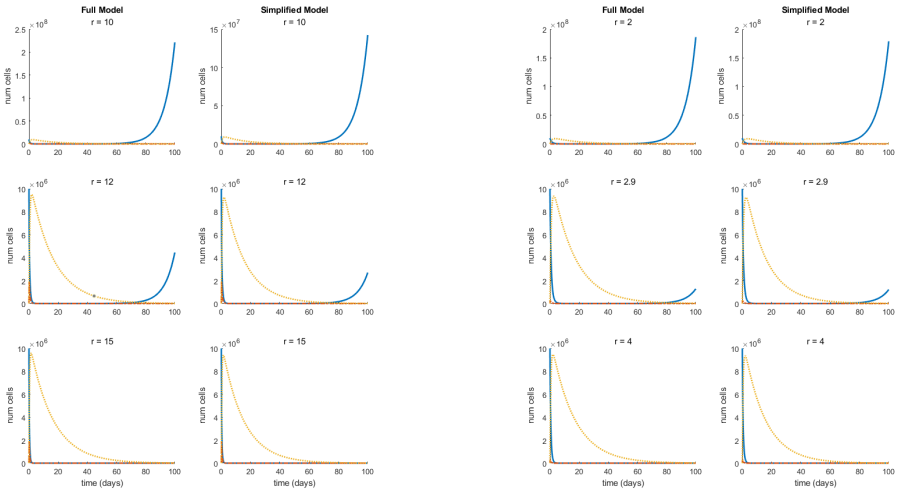

Patu-8988T Dan-G

Figure 5: Populations of healthy cells (solid line -), sub-lethally damaged cells (dot-dashed line -.), and doomed cells (dotted line :) for different values of r using the uptake radiation curve ($\lambda_s = 0.139, \lambda_d = 5.55 \cdot 10^{-3}$).

4 Stochastic extension

4.1 Formulation

We now turn to extending the general model above to a stochastic differential equation (SDE). We will follow the process as described by section 9.3 of Allen (2010). Consider the possible interactions that can occur between the three populations in Figure 6 and denote the process described by the model as $\mathcal{N}(t)$.

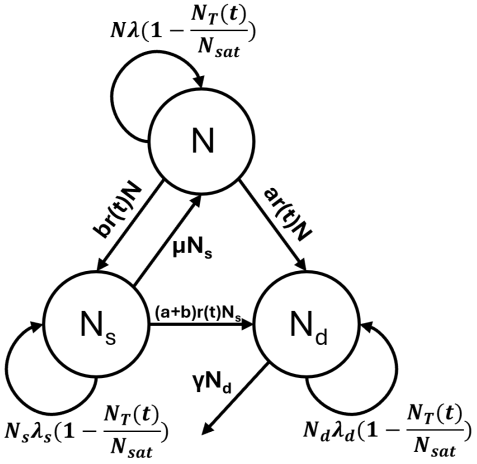

i	Change, $(\Delta\mathcal{N}(t))_i$	Probability, p_i
1	$[1,0,0]^{tr}$	$\lambda N\left(1-\frac{N_T}{N_{sat}}\right)\Delta t$
2	$[0,1,0]^{tr}$	$\lambda_s N_s\left(1-\frac{N_T}{N_{sat}}\right)\Delta t$
3	$[0,0,1]^{tr}$	$\lambda_d N_d\left(1-\frac{N_T}{N_{sat}}\right)\Delta t$
4	$[1,-1,0]^{tr}$	$\mu N_s\Delta t$
5	$[-1,1,0]^{tr}$	$br(t)N\Delta t$
6	$[-1,0,1]^{tr}$	$ar(t)N\Delta t$
7	$[0,-1,1]^{tr}$	$(a+b)r(t)N_s\Delta t$
8	$[0,0,-1]^{tr}$	$\gamma N_d\Delta t$

Figure 6: Schematic diagram of the transitions between different populations of cells in the full model. Here $N_T(t) \coloneqq N(t) + N_s(t) + N_d(t)$.

First we compute the expectation $\mathbb{E}[\Delta\mathcal{N}]$.

$$\mathbb{E}[\Delta\mathcal{N}] = \sum_i p_i(\Delta\mathcal{N})_i = \begin{bmatrix} \lambda N\left(1-\frac{N_T}{N_{sat}}\right) + \mu N_s - (a+b)r(t)N \\ \lambda_s N_s\left(1-\frac{N_T}{N_{sat}}\right) + br(t)N - \mu N_s - (a+b)r(t)N_s \\ \lambda_d N_d\left(1-\frac{N_T}{N_{sat}}\right) + (a+b)r(t)N_s - \gamma N_d + ar(t)N \end{bmatrix}\Delta t \tag{26}$$

Next we compute the covariance matrix for $\mathcal{N}(t)$.

$$\Sigma(\Delta\mathcal{N}) = \begin{bmatrix} \mathrm{Cov}(N,N) & \mathrm{Cov}(N_s,N) & \mathrm{Cov}(N_d,N) \\ \mathrm{Cov}(N,N_s) & \mathrm{Cov}(N_s,N_s) & \mathrm{Cov}(N_d,N_s) \\ \mathrm{Cov}(N,N_d) & \mathrm{Cov}(N_s,N_d) & \mathrm{Cov}(N_d,N_d) \end{bmatrix}\Delta t = V\Delta t \tag{27}$$

Using the definition of the covariances,

$$\Sigma(\Delta\mathcal{N}) = \sum_i p_i(\Delta\mathcal{N})_i(\Delta\mathcal{N})_i^{tr} \tag{28}$$

we compute each covariance as

$$\mathrm{Cov}(N,N) = \lambda N\left(1-\frac{N_T}{N_{sat}}\right) + \mu N_s + (a+b)r(t)N \tag{29}$$

$$\mathrm{Cov}(N_s,N_s) = \lambda_s N_s\left(1-\frac{N_T}{N_{sat}}\right) + \mu N_s + (a+b)r(t)N_s + br(t)N \tag{30}$$

$$\mathrm{Cov}(N_d,N_d) = \lambda_d N_d\left(1-\frac{N_T}{N_{sat}}\right) + (a+b)r(t)N_s + \gamma N_d + ar(t)N \tag{31}$$

$$\mathrm{Cov}(N,N_s) = -\mu N_s - br(t)N \tag{32}$$

$$\mathrm{Cov}(N,N_d) = -ar(t)N \tag{33}$$

$$\mathrm{Cov}(N_s,N_d) = -(a+b)r(t)N_s \tag{34}$$

Let the matrix $S \coloneqq \sqrt{V}$, where V is from equation (27). Then from equation 9.7 in Allen,

$$d\mathcal{N}(t) = \frac{\mathbb{E}[\mathcal{N}(t)]}{\Delta t}dt + S(\mathcal{N}(t), t)dW(t) \tag{35}$$

where $dW(t)$ is the derivative of the Wiener process. If we consider excluding the stochastic elements from equation (35), then we have that

$$d\mathcal{N}(t) = \frac{\mathbb{E}[\mathcal{N}(t)]}{\Delta t}dt \implies \begin{bmatrix} dN \\ dN_s \\ dN_d \end{bmatrix} = \begin{bmatrix} \lambda N\left(1 - \frac{N_T}{N_{sat}}\right) + \mu N_s - (a+b)r(t)N \\ \lambda_s N_s\left(1 - \frac{N_T}{N_{sat}}\right) + br(t)N - \mu N_s - (a+b)r(t)N_s \\ \lambda_d N_d\left(1 - \frac{N_T}{N_{sat}}\right) + ar(t)N + (a+b)r(t)N_s - \gamma N_d \end{bmatrix} dt \tag{36}$$

which shows that the mean of the SDEs agree exactly with the deterministic ODE model presented in equations (1), (2), and (3). We then have the following system of stochastic differential equations:

$$dN(t) = \lambda N\left(1 - \frac{N_T}{N_{sat}}\right) + \mu N_s - (a+b)r(t)N + S_{1,1}dW_1(t) + S_{1,2}dW_2(t) + S_{1,3}dW_3(t) \tag{37}$$

$$dN_s(t) = \lambda_s N_s\left(1 - \frac{N_T}{N_{sat}}\right) + br(t)N - \mu N_s - (a+b)r(t)N_s + S_{2,1}dW_1(t) + S_{2,2}dW_2(t) + S_{2,3}dW_3(t) \tag{38}$$

$$dN_d(t) = \lambda_d N_d\left(1 - \frac{N_T}{N_{sat}}\right) + ar(t)N + (a+b)r(t)N_s - \gamma N_d + S_{3,1}dW_1(t) + S_{3,2}dW_2(t) + S_{3,3}dW_3(t) \tag{39}$$

where $W_1(t)$, $W_2(t)$, and $W_3(t)$ are three independent Wiener processes.

We attempted to compute the square root of matrix V explicitly using Mathematica; however, the total size of the resultant matrix S in memory was 162.7MB. After substituting parameter values to match Dan-G cells and setting $\lambda_s = 0.139, \lambda_d = 5.55 \cdot 10^{-3}$, the matrix size was still 36.5MB, with $S_{1,1}$ occupying 3.9MB alone. It is thus infeasible for the scope of this report to deal with this matrix directly.

4.2 Modeling

Since S could not be computed directly, we attempted to model this SDE numerically via MATLAB. First we tried substituting all the values for parameters and N, N_s, and N_d, and only then computing the square root matrix S using MATLAB's `sqrtm()` method. This implementation can be seen in `sde_1.m`. This attempt was a failure; the matrix V eventually contained an infinite element and the square root could not be computed. Instead, we tried to inject stochasticity into the deterministic model code we used for the earlier modeling by computing S and the Wiener process product at each time step in `ode45`. This also ended in failure as the matrix V eventually became singular and again could not have the square root computed. This attempt can be see in `sde_2.m`.

As a last resort, we tried to model the equations stochastically using Gilesspi simulations. We considered the eight different possible transitions as shown in Figure 6 and at each time step computed the set of probabilities and selected one event to occur via a weighted random. This also did not perform as expected, and all populations grew linearly. This final implementation can be seen in `sde_3.m`.

5 Conclusions

In conclusion, for the parameter sets that were tested in this report, the simplified model that Neira, Gago-Arias, Guiu-Souto, and Pardo-Montero (2020) described mimicked the behavior of the general model almost exactly. As seen from the fixed point analysis, despite the simplified model compressing fixed curves down to single points, these fixed points followed the fixed curves. This kept the dynamics of the two models almost exact, so that no qualitative changes occurred in one but not the other. Additionally, for both models the

computed bifurcation value r of the radiation for the fixed point at the origin remained the same. In light of this, our conclusion is that the simplified model that the authors used is a good approximation of the general model.

One may wonder, however, what benefit is gained from this simplification. In our simulations, both models were simulated in an equivalent duration of time, so the computation time saved by considering the simplified model is negligible. One possible advantage of the simplified is that in some computations, the results of the simplified model were nicer than the general, but this is a minor advantage at best.

On the other hand, the LQ limit reduction the authors performed does not accurately reflect the behavior of either the general or simplified models. The LQ limit version has a single fixed point at the origin that remains an attractor for all feasible values for a, b, and r. Under this, with only the slightest presence of radiation that would not deter the general model, the LQ limit will predict that the tumor will be eventually eradicated. This makes the LQ model an inadequate reduction, and one may wonder what insight is gained through their comparison to the LQ model (Lea and Catcheside 1942, Kellerer and Rossi 1974, Fowler 1989).

Lastly, we completed our goal of computing an equivalent set of stochastic differential equations for the general model, but we failed to simulate these equations numerically despite three different attempts. The variance matrix revealed itself to be much larger than anticipated, rendering it unwieldy. Additionally, the matrix V in two of our simulation attempts either contained infinite entries or became singular, preventing successful simulation.

5.1 Further extensions

The results for this paper are confined to only two cell lines and two sets of parameter values for λ_s and λ_d. This means that the results presented are applicable only for a narrow set of the total parameter space, and must be treated as such. A valuable further insight would be evaluating the general and simplified models for a larger set of parameters from many more types of cells.

As seen by our *ad hoc* investigation of the sub-lethal repair parameter μ, the rate at these cells repair themselves affects the bifurcation value for r at the origin. An interesting extension would be to investigate how exactly μ affects the stability of the origin. Perhaps there is a biological way to change the repair rate of these cells, via inhibitors or otherwise, that would allow the healthy cells to be attracted to the origin without varying the amount of radiation in the patient's system.

Additionally, the modeling of the SDEs in this report remains unfinished. It would be pertinent to successfully model these equations to see how the models develop under stochasticity.

Supplemental material

We include here results that are either too long to display or not immediately relevant to the body of the paper but whose results are mentioned. The full code and set of results for this paper can be viewed in the github repository at `https://github.com/rbottoms18/TumorModelInvestigation`.

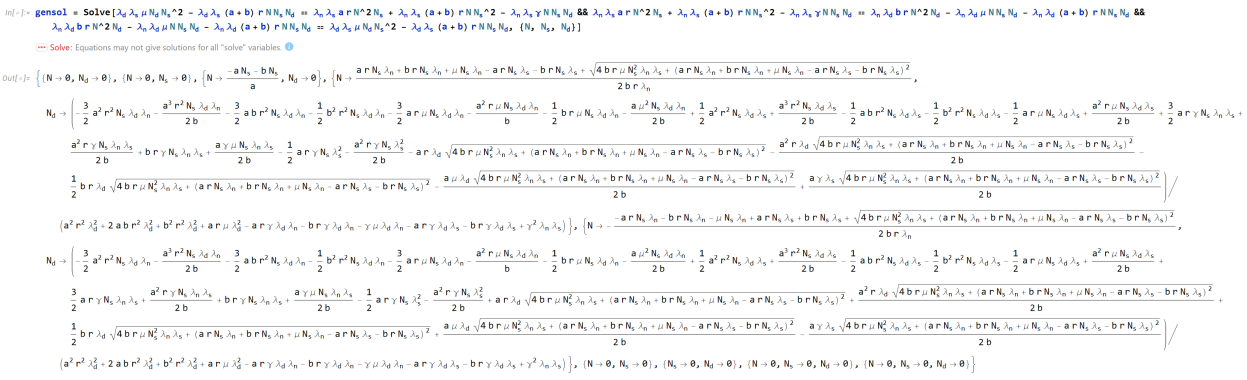

Figure 7: Fixed points and curves of the general model. Observe that there are two fixed curves that depend on the number of sub-lethally damaged cells.

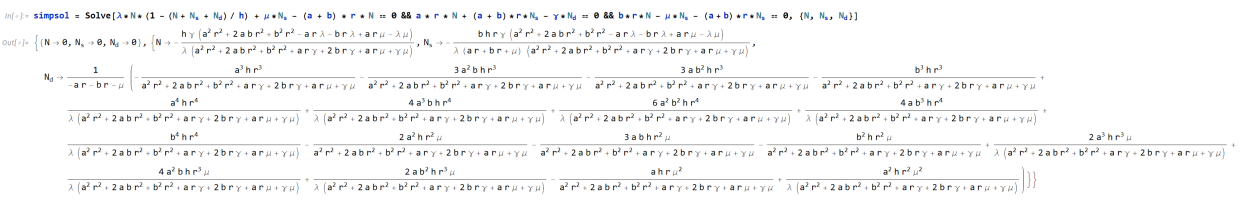

Figure 8: Fixed points of the simplified model. Observe that the two fixed curves of the general model have been collapsed into two stationary fixed points.

Acknowledgements

I would like to acknowledge Professor Mamis for his enthusiastic support and for his generous input and aid on not only the mathematics behind the analyses, but on implementations and suggestions on coding the simulations. The effect of his support for the process of research and writing of this paper cannot be understated.

References

Allen, Linda J.S. An Introduction to Stochastic Processes with Applications to Biology. 2nd ed., Chapman and Hall, 2010.

Baiu D C *et al* 2018 Targeted molecular radiotherapy of pediatric solid tumors using a radioiodinated alkyl-phospholipid ether analog *J. Nucl. Med* **59** 244-50

Curtis S B 1986 Lethal and potentially lethal lesions induced by radiation – a unified repair model *Radiat. Res.* **106** 252-70

Fowler J F 1989 The linear-quadratic formula and progress in fractionated radiotherapy *Br. J. Radiol.* **62** 679-94

Gago-Arias, A.; Neira, S.; Terragni, F.; Pardo-Montero, J. A Mathematical Model of Thyroid Disease Response to Radiotherapy. *Mathematics* **2021**, *9(19)*, 2365

Kellerer A M and Rossi H H 1974 The theory of dual radiation action *Curr. Top. Radiat. Res.* **8** 85-158

Lea D E and Catcheside D G 1942 The mechanism of the induction by radiation of chromosome aberrations in *Tradescantia J. Genet.* **44** 216-45

Neira, S.; Gago-Arias, A.; Guiu-Souto, J.; Pardo-Montero, J. A kinetic model of continuous radiation damage to populations of cells: Comparison to the LQ model and application to molecular radiotherapy. *Phys. Med. Biol.* **2020**, *65*, 245015.